

Model Inversion of a Two Degrees of Freedom Linearized PUMA from Bicausal Bond Graphs

Gilberto Gonzalez-A, Ignacio Rodríguez- A., Dunia Nuñez-P

Abstract—A bond graph model of a two degrees of freedom PUMA is described. System inversion gives the system input required to generate a given system output. In order to get the system inversion of the PUMA manipulator, a linearization of the nonlinear bond graph is obtained. Hence, the bicausality of the linearized bond graph of the PUMA manipulator is applied. Thus, the bicausal bond graph provides a systematic way of generating the equations of the system inversion. Simulation results to verify the calculated input for a given output are shown.

Keywords—Bond graph, system inversion, bicausality, PUMA manipulator

I. INTRODUCTION

ROBOTICS is a field of modern technology that crosses traditional engineering boundaries. Understanding the complexity of robots and their applications requires knowledge of electrical engineering, mechanical engineering, industrial engineering, computer science and mathematics [1].

One well-known approach designed to deal with multi-domain engineering problems is the bond graph method elucidated by Henry Paynter. The application of Paynter's bond graph method began with the works of Karnopp, Rosenberg, Thoma and others. Over the last 40 years there have been numerous publications dealing with the theory and application of bond graphs in different branches of engineering [2].

The bond graph technics are useful and important tools for physical system modelling [3]. They are based on power representation and enables the description of the system through energy storage and dissipative elements [4], [5].

The robotics modelling using bond graphs has extensively been developed. In [3] proposes a general methodology to model mechanical systems with bond graphs. In [6] presents an interesting procedure to construct bond graphs of two and three dimensional robotic manipulators. The three-axis platform simulation using bond graph models and Lagrange's equations is compared in [7].

Also, several papers have been published to construct bond graphs from the manipulators. In [8] gives a library of three-dimensional joints using bond graph to obtain the multi-body system. Finally, [9] shows the multi-body approach in bond graph to write the algebraic constraint equations can be used to describe mechanical systems.

Gilberto Gonzalez-A is with the Faculty of Electrical Engineering, University of Michoacan (e-mail: gilmichga@yahoo.com.mx)

Ignacio Rodríguez-A is with the Faculty of Electrical Engineering, University of Michoacan

Dunia Nuñez-P is with Faculty of Electrical Engineering, University of Michoacan

System inversion is of significant importance in systems and control theory as it appears explicitly or implicitly in a variety of problems such as, for example, decoupling, model matching, perfect output control or parameters sizing [10].

Classical inversion methods based on mathematical models tend to obscure the structural features and the physical interpretation of inverse systems. In recent years, bond graph model based inversion has attracted a lot of interest due to the bicausality concept that provides a convenient way to represent inverse systems [11].

The main advantage for using bond graphs for such study is the graphical representation of the physical structure of the system as well as the possible automated derivation of various equations (or mathematical) models that can be associated with a specific problem of interest through the causality assignment. This bond graph approach therefore enables a physical interpretation of inverse dynamics based on structural considerations [12].

Section II describes the basic elements of the bond graph modelling. Section III summarizes the concept of the bicausality applied to bond graphs. Bicausality used to get systems inversion is proposed in section IV. The given methodology to a two degrees of freedom PUMA manipulator modelled by a linearized bond graph to determine the control inputs for proposed outputs via bicausality is applied in section V. Finally, our conclusions are given in section VI.

II. MODELING IN BOND GRAPH

The symbolic form of a Bond Graph in Integral causality assignment (BGI) of a system is shown in Fig. 1 [4], [5].

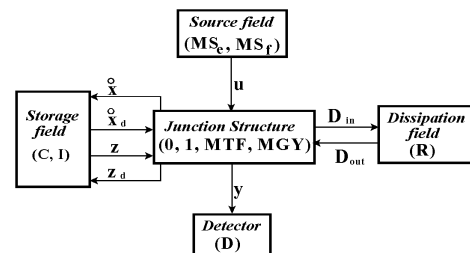


Fig. 1 Key vectors of a BGI

In Fig. 1, (MS_e, MS_f) , (C, I) and (R) denote the source, the energy storage and the energy dissipation fields, and $(0, 1, MTF, MGY)$ the junction structure with transformers, MTF , and gyrators, MGY .

The state $x(t) \in \mathfrak{R}^n$ and $x_d(t) \in \mathfrak{R}^m$ are composed of energy variables $p(t)$ and $q(t)$ associated with I and C elements in integral and derivative causality, respectively $u(t) \in \mathfrak{R}^p$ denotes the plant input, $z(t) \in \mathfrak{R}^n$ the co-energy vector, $z_d(t) \in \mathfrak{R}^m$ the derivative causality and $D_{in}(t) \in \mathfrak{R}^r$ and $D_{out}(t) \in \mathfrak{R}^r$ are a mixture of $e(t)$ and $f(t)$ showing the energy exchanges between the dissipation field and the junction structure.

The relations of the storage and dissipation field are,

$$z(t) = Fx(t) \tag{1}$$

$$z_d(t) = F_d x_d(t) \tag{2}$$

$$D_{out}(t) = LD_{in}(t) \tag{3}$$

The relations of the junction structure are,

$$\begin{bmatrix} \dot{x}(t) \\ D_{in}(t) \\ y(t) \\ z_d(t) \end{bmatrix} = \begin{bmatrix} S_{11} & S_{12} & S_{13} & S_{14} \\ S_{21} & S_{22} & S_{23} & 0 \\ S_{31} & S_{32} & S_{33} & 0 \\ S_{41} & 0 & 0 & 0 \end{bmatrix} \begin{bmatrix} z(t) \\ D_{out}(t) \\ u(t) \\ \dot{x}_d(t) \end{bmatrix} \tag{4}$$

The entries of S take values inside the set $\{0, \pm 1, \pm K_t, \pm K_g\}$

where K_t and K_g are transformer and gyrator modules; S_{11} and S_{22} are square skew-symmetric matrices and S_{12} and S_{21} are matrices each other negative transpose. The state equation is [4], [5],

$$\dot{x}(t) = A(x)x(t) + B(x)u(t) \tag{5}$$

$$y(t) = C(x)x(t) + D(x)u(t) \tag{6}$$

where

$$EA(x) = \left[S_{11} + S_{12}MS_{21} + S_{14}F_d^{-1} \frac{dS_{31}}{dt} \right] F \tag{7}$$

$$EB(x) = S_{13} + S_{12}MS_{23} \tag{8}$$

$$C(x) = (S_{31} + S_{32}MS_{21})F \tag{9}$$

$$D(x) = S_{33} + S_{32}MS_{23} \tag{10}$$

being

$$M = (I - LS_{22})^{-1}L \tag{11}$$

$$E = I - S_{14}F_d^{-1}S_{31}F \tag{12}$$

Next section describes bicausal bond graphs to analyze system inversion.

III. THE CONCEPT OF THE BICAUSAL BOND GRAPH

The acausal bond graph model of a dynamic system represents the energy transfer and the constraint equations in the system independently of assignment statements that can be derived from those equations.

The causality expresses in which way constitutive relations of elements and relations among variables of the junction structure should be written for model analysis proposes or derivation of a simulation model. The causal stroke used in conventional bond graphs basically supposes that at each bond, if the effort (resp. flow) is imposed at the other end of

the bond or in other words a variable imposed as input implies its conjugate variable as output.

From a computational point of view, the above so-called 'unicausal' stroke does not determine all forms of assignment statements that can be derived from the constraint equations of a bond.

The concept of 'bicausal' bond introduced by Gwathrop [11] overcomes these restrictions and then enlarges the possibilities of computation models that can be derived from a bond graph.

The causal stroke in bicausal bond is seen as half strokes each associated to an effort and a flow variable that can be imposed independently at each end of the bond. Causal half strokes indicate the fixed or known variables of the bond and so determine the right hand side of the assignments form.

For an illustration, Table 1 [12] presents assignment statements associated to unicausal and bicausal strokes for a bond for which the known acausal constraint equations are: $e_1 - e_2 = 0$; $f_1 - f_2 = 0$.

TABLE I
CAUSALITY AND ASSIGNMENT STATEMENTS FOR A BOND

Unicausal Stroke	Assignment Statements	Bicausal Stroke	Assignment Statements
	$e_2 := e_1$ $f_1 := f_2$		$e_1 := e_2$ $f_1 := f_2$
	$e_1 := e_2$ $f_2 := f_1$		$e_2 := e_1$ $f_2 := f_1$

TABLE II
SOURCE-SENSOR CAUSALITY ASSIGNMENT

Unicausal Stroke	SS Element Type	Bicausal Stroke	SS Element Type
	Flow source/ effort sensor		Flow source/ effort source
	Effort source/ flow sensor		Flow sensor/ effort sensor

System inversion is an interesting analysis to know an input considering a given output, this is described in the next section by using bicausality property of the bond graphs.

IV. THE USE OF THE BICAUSALITY CONCEPT FOR SYSTEM INVERSION

An inverse model of the system are obtained by applying differential and algebraic operations to the state equations of the original system. The computational capabilities of the bicausality concept presented above make it be an adequate tool for solving the problem of inverse systems mentioned in [11]. The bicausality allows fixing or imposing at the same time a variable and its conjugate as bicausal bonds decouple the effort and flow causalities. In the context of the inversion problem, imposing the output variable without modifying the energy structure (or constraint equations) of the system can be carried out with an SS element having a flow source/effort source causality (Table II). Then, the output to be imposed plays the role of input variable of that SS element while its conjugate is set to a null value leading to a null power flow on that bond.

Similarly, the input variable of the original system to be determined will be detected on another SS element with a flow sensor/effort sensor causality. Table III shows the bicausality propagation carried out throughout junction structure of the bond graph.

TABLE III
CAUSALITY STROKE AND ASSIGNMENT STATEMENTS FOR BOND GRAPH ELEMENT

Unicausal Stroke	Assignment Statements	Bicausal Stroke	Assignment Statements
	$f:=e/R$ $e:=R*f$		$R:=e/f$
	$f:=p/I$ $p:=I*f$		$I:=p/f$
	$q:=C*e$ $e:=q/C$		$C:=q/e$
	$e2:=e1/n$ $f1:=f2/n$		$e1:=n*e2$ $f1:=f2/n$
	$e1:=n*e2$ $f2:=n*f1$		$e2:=e1/n$ $f2:=n*f1$
	$f1:=e2/r$ $f2:=e1/r$		$e1:=r*f2$ $f1:=e2/r$
	$e1:=r*f2$ $e2:=r*f1$		$e2:=r*f1$ $f2:=e1/r$
	$e2:=e1$ $e3:=e1$ $f1:=f2+f3$		$e2:=e1$ $e3:=e1$ $f3:=f1-f2$
	$f2:=f1$ $f3:=f1$ $e1:=e2+e3$		$f2:=f1$ $f3:=f1$ $e3:=e1-e2$

Some concepts used to present the bond graph-based procedure for system inversion are introduced in this section through the following definitions [12].

Definition 1. The length L_k of a causal path from a variable v_i to a variable v_j of a bond graph is defined as the number of integrators or storage elements in integral causality encountered on the causal path when following the causal path from v_i to v_j .

Proposition 1. (Structural invertibility condition) A linear system modelled by bond graph is invertible if there is at least one causal path between the input variable and the output variable of the system.

In the next section, a bond graph model of a PUMA manipulator and system inversion are proposed.

V. ANALYSIS OF A TWO DEGREES OF FREEDOM PUMA WITH A BOND GRAPH APPROACH

A simple two-degrees of freedom (DOF) manipulator but three-dimensional appears in Fig. 2. This can be regarded as a simplified PUMA with the elbow and wrist locked at appropriate angles and zero joint offset.

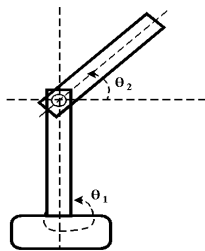


Fig. 2 Scheme of 2 DOF PUMA

The second link, although moving in three dimensions, rotates about a fixed point: joint 2. Its dynamics are therefore determined by the Euler ring. The first link is a simple one-dimensional rotating inertia coupled to the second link by a joint [6]. The angular velocities of the second link about the x and y axes w_x and w_y are entirely determined by that of the first link w_1 ,

$$w_x = w_1 \cdot \sin(\theta_2) \tag{13}$$

$$w_y = w_1 \cdot \cos(\theta_2) \tag{14}$$

The corresponding bond graph with integral causality assignment of the PUMA manipulator is shown in Fig. 3 with notation in Table 4.

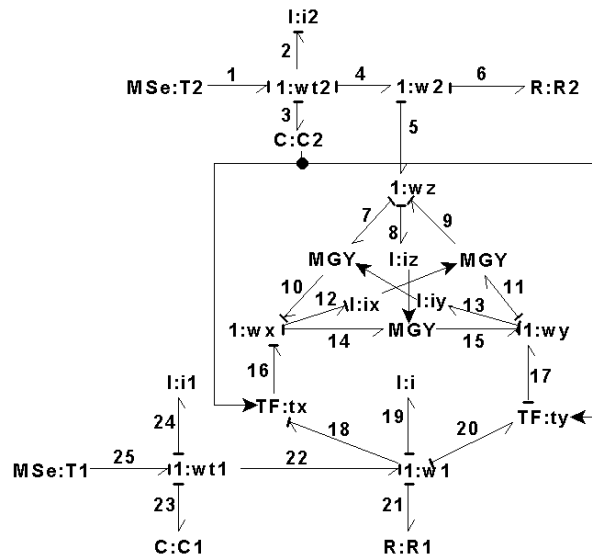


Fig. 3 Bond graph of the PUMA manipulator

Note that the bond graph contains four storage element in an integral causality assignment, that is independent linearly state variables.

TABLE IV
BOND GRAPH LABELS

Label	Component type	Associated physical variable
wt1, wt2	Common velocity junctions	Joint angular velocities $\dot{\theta}_1, \dot{\theta}_2$
wx, wy, wz	Common velocity junctions	Angular velocities wx, wy, wz
i1	Inertia component	Inertia of link 1
ix, iy, iz	Inertia components	Principle angular momenta hx, hy, hz
gx, gy, gz	Gyrators	Coupling due to rotating coordinate system
T1, T2	Sources	Torques T1, T2
tx, ty	Transformers	Transformations of the second link
C	Compliance component	Provides the joint angle θ_2

The key vectors of the nonlinear bond graph are,

$$x = \begin{bmatrix} p_2 \\ p_{24} \\ q_3 \\ q_{23} \end{bmatrix}; \dot{x} = \begin{bmatrix} e_2 \\ e_{24} \\ f_3 \\ f_{23} \end{bmatrix}; z = \begin{bmatrix} f_2 \\ f_{24} \\ e_3 \\ e_{23} \end{bmatrix}$$

$$x_d = \begin{bmatrix} p_8 \\ p_{12} \\ p_{13} \\ p_{19} \end{bmatrix}; \dot{x}_d = \begin{bmatrix} e_8 \\ e_{12} \\ e_{13} \\ e_{19} \end{bmatrix}; z_d = \begin{bmatrix} f_8 \\ f_{12} \\ f_{13} \\ f_{19} \end{bmatrix}$$

$$D_m = \begin{bmatrix} f_6 \\ f_{21} \end{bmatrix}; D_{out} = \begin{bmatrix} e_6 \\ e_{21} \end{bmatrix}$$

$$u = \begin{bmatrix} e_1 \\ e_{25} \end{bmatrix}; y = \begin{bmatrix} f_3 \\ f_{23} \end{bmatrix}$$

$$EA(x) = \begin{bmatrix} -R_2 & -h_1 & -1 & 0 \\ i_2 & i_1 & C_1 & 0 \\ h_1 & -R_1 & 0 & -1 \\ i_1 & i_1 & 0 & C_1 \\ \frac{1}{i_2} & 0 & 0 & 0 \\ 0 & \frac{1}{i_1} & 0 & 0 \end{bmatrix}$$

$$EB(x) = \begin{bmatrix} 1 & 0 & 0 & 0 \\ 0 & 1 & 0 & 0 \end{bmatrix}^T$$

It is an unfortunate fact that most physical systems encountered in practice are not linear. It is almost always the case that when one encounters a linear model for a physical system, it is an idealized or simplified version of a more accurate but much more complicated nonlinear model. In order to create a linear model of the PUMA manipulator represented in bond graph from the nonlinear bond graph shown in figure 3, we introduce a linearized bond graph of the manipulator in figure 4 [13].

the constitutive relations of the fields are

$$F = \text{diag} \left\{ \frac{1}{i_2}, \frac{1}{i_1}, \frac{1}{C_2}, \frac{1}{C_1} \right\}$$

$$F_d = \text{diag} \left\{ \frac{1}{i_z}, \frac{1}{i_x}, \frac{1}{i_y}, \frac{1}{i} \right\}$$

and the junction structure matrices are

$$S_{11} = \begin{bmatrix} 0 & -h_1 & -1 & 0 \\ h_1 & 0 & 0 & -1 \\ 1 & 0 & 0 & 0 \\ 0 & 1 & 0 & 0 \end{bmatrix}; S_{12} = \begin{bmatrix} -1 & 0 \\ 0 & -1 \\ 0 & 0 \\ 0 & 0 \end{bmatrix}$$

$$S_{14} = \begin{bmatrix} -1 & 0 & 0 & 0 \\ 0 & -\sin(q_3) & -\cos(q_3) & -1 \\ 0 & 0 & 0 & 0 \\ 0 & 0 & 0 & 0 \end{bmatrix}$$

$$S_{13} = \begin{bmatrix} 1 & 0 & 0 & 0 \\ 0 & 1 & 0 & 0 \end{bmatrix}^T$$

$$S_{22} = S_{23} = 0; S_{21} = -S_{12}^T; S_{31} = -S_{14}^T$$

where $h_1 = p_{13} \sin(q_3) - p_{12} \cos(q_3)$.

From

$$E = \begin{bmatrix} 1 + \frac{i_z}{i_2} & 0 & 0 & 0 \\ 0 & 1 + h_2 & 0 & 0 \\ 0 & 0 & 1 & 0 \\ 0 & 0 & 0 & 1 \end{bmatrix}$$

where $h_2 = \frac{1}{i_1} [i_x \cos^2(q_3) + i_y \sin^2(q_3) + i]$

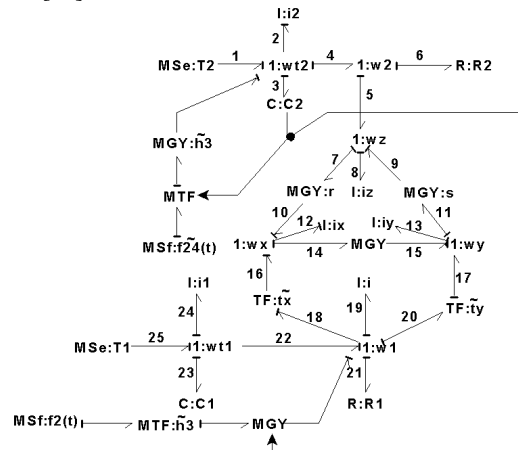


Fig. 4 Linearized bond graph

In order to verify that linearized bond graph represents the linearization of the nonlinear manipulator, the junction structure matrix of the linearized bond graph or causal paths to obtain the state variables description can be used. The space state representation of a linearized system is

$$E_\delta \dot{x}_\delta(t) = A_\delta x_\delta(t) + B_\delta u_\delta(t)$$

Hence, the state variables matrices are

$$E_\delta = \text{diag} \left\{ 1 + \frac{i_z}{i_2}, 1 + \frac{i_x + i}{i_1}, 1, 1 \right\}$$

$$A_{\delta} = \begin{bmatrix} -R_2 & -\tilde{h}_1 & -1 & -\tilde{h}_3 f_{29} & 0 \\ \frac{1}{i_2} & \frac{1}{i_1} & C_2 & 0 & 0 \\ \tilde{h}_1 & -R_1 & \tilde{h}_3 f_{29} & -1 & 0 \\ \frac{1}{i_2} & 0 & 0 & C_1 & 0 \\ 0 & \frac{1}{i_1} & 0 & 0 & 0 \end{bmatrix}; B_{\delta} = \begin{bmatrix} 1 \\ 1 \\ 0 \\ 0 \end{bmatrix}$$

where $\tilde{h}_1 = h_{1\tilde{x}(t)}$, $\tilde{h}_3 = h_{3\tilde{x}(t)}$ and $h_3 = p_{13} \cos(q_3) + p_{12} \sin(q_3)$

By obtaining the direct paths, i.e., causal paths from input to output, we have

$$u_1 \rightarrow y_1 : e_{25} - e_{24} - f_{24}$$

$$u_2 \rightarrow y_2 : e_1 - e_2 - f_2$$

then these causal paths are of length 1 and the structural invertibility condition is verified.

Now, bicausality to the linearized bond graph of the PUMA manipulator is applied to get a system inversion. Fig. 5 shows the bicausal bond graph of the PUMA manipulator.

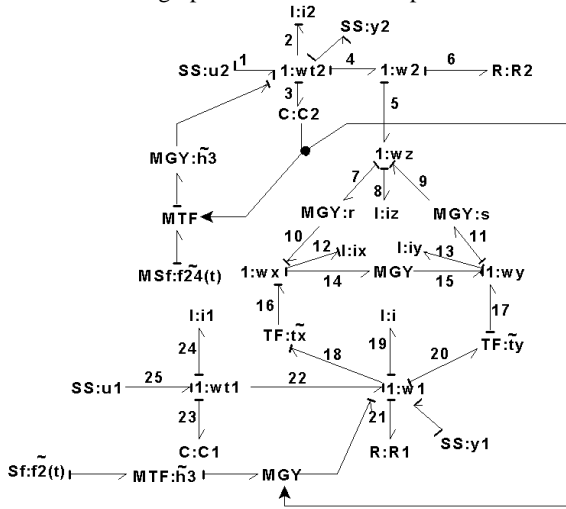


Fig. 5 Bicausal bond graph of the manipulator

The generalized state equations of the inverse model derived from the inverse bond graph in Fig. 5 can be written in a descriptor form or alternatively in the following generalized state equations form:

$$\dot{z}(t) = Fz(t) + G(p)y(t)$$

$$u(t) = Hz(t) + J(p)y(t)$$

where

$$z^T(t) = [qc_1 \quad qc_2]; F = 0$$

$$G(p) = \begin{bmatrix} 1 & 0 \\ 0 & 1 \end{bmatrix}$$

and the causal paths are used to get H and $J(p)$. Then,

Causal path $y_2 \rightarrow u_2$	Gain
$f_2 - f_4 - f_6 - e_6 - e_4 - e_1$	R_2
$f_2 - f_3 - e_3 - e_1$	$1/C_2$

$f_2 - f_4 - f_5 - f_8 - e_8 - e_5 - e_4 - e_1$	I_z
$f_2 - f_2 - e_2 - e_1$	I_2

Causal path $y_1 \rightarrow u_1$	Gain
$f_{23} - f_{22} - f_{21} - e_{21} - e_{22} - e_{25}$	R_1
$f_{23} - f_{24} - e_{24} - e_{25}$	$1/C_1$
$f_{23} - f_{22} - f_{19} - e_{19} - e_{22} - e_{25}$	I_y
$f_{23} - f_{23} - e_{23} - e_{25}$	I_1

Causal path $y_1 \rightarrow u_2$	Gain
$f_{23} - f_{22} - f_{20} - f_{17} - e_9 - e_5 - e_4 - e_1$	$k_2 s$
$f_{23} - f_{22} - f_{18} - f_{16} - f_{10} - e_7 - e_5 - e_4 - e_1$	$k_1 r$

Causal path $y_2 \rightarrow u_1$	Gain
$f_2 - f_4 - f_5 - f_9 - e_{11} - e_{17} - e_{20} - e_{22} - e_{25}$	$k_2 s$
$f_2 - f_9 - f_5 - f_7 - e_{10} - e_{16} - e_{18} - e_{22} - e_{25}$	$k_1 r$

Thus, the input of the system inversion is given by

$$u(t) = \begin{bmatrix} \frac{1}{C_1} & 0 \\ 0 & \frac{1}{C_2} \end{bmatrix} z(t) + \begin{bmatrix} \alpha_{11} & \alpha_{12} \\ \alpha_{21} & \alpha_{22} \end{bmatrix} \begin{bmatrix} y_1(t) \\ y_2(t) \end{bmatrix}$$

where

$$\alpha_{11} = \left(\frac{1}{C_1} + R_1 + I_y \right) + \frac{dl_1}{dt}$$

$$\alpha_{12} = k_1 r + k_2 s$$

$$\alpha_{21} = k_1 r - k_2 s$$

$$\alpha_{22} = \left(\frac{1}{C_2} + R_2 + I_z \right) + \frac{dl_2}{dt}$$

In order to verify the system inversion of the manipulator, the 20-SIM software to simulate linearized bond graph with a calculated control input is used. Figure 6 shows the bond graph diagram on 20-SIM platform.

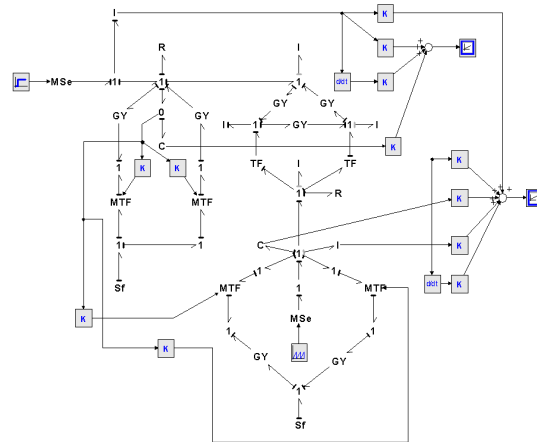


Fig. 6 Bond graph of the manipulator on 20-SIM

The numerical parameters of the bond graph are:

$$C_1 = 0.1 \text{rad} / N - m, \quad C_2 = 0.2 \text{rad} / N - m, \quad I_1 = 0.1 N - m - s^2, \\ I_2 = 0.2 N - m - s^2, \quad I = I_z = I_x = I_y = 1 N - m - s^2, \quad R_1 = 4 N - s / m \\ \text{and } R_2 = 3 N - s / m.$$

The first case is to determine the necessary inputs for step outputs and Fig. 7 shows the simulation results.

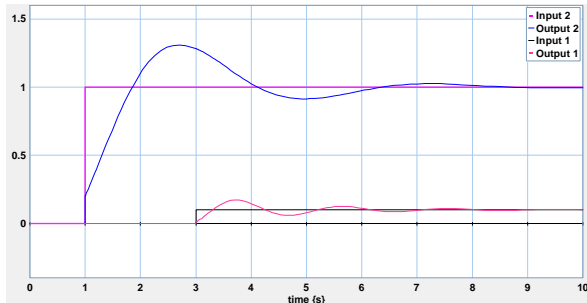


Fig. 7 Simulation of the system inversion for step outputs

The second case is to prove the system inversion for waves square outputs, the effectiveness of the methodology is shown in Fig. 8.

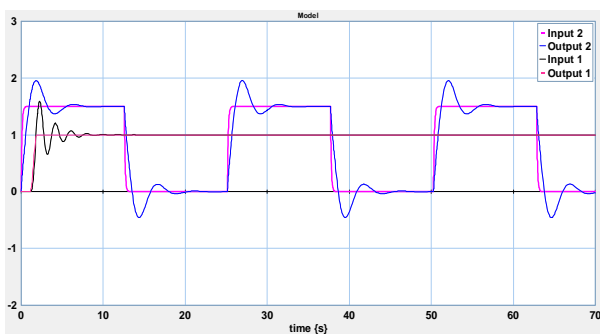


Fig. 8 Simulation of the system inversion for waves square

Fig. 9 shows the final proof of the system inversion using waves saw outputs and the necessary inputs are obtained

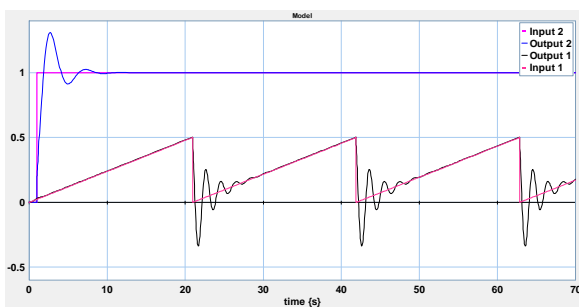


Fig. 9 Simulation of the system inversion

It is important to consider the bond graph bicausals allows to determine system inversion state estimation and parameter estimation [11].

VI. CONCLUSIONS

The bond graph representation and the concept of bicausality are used to obtain the system inversion of a PUMA manipulator. Hence, the nonlinear bond graph of the two degrees of freedom PUMA is linearized. Then, the linearized bond graph bicausal is obtained. Thus, the system input to get a given system output of the linearized PUMA is determined in a bond graph approach.

REFERENCES

- [1] Mark W. Spong and M. Vidyasagar, "Robot Dynamics and Control", John Wiley & Sons, 1989.
- [2] V. Damic and J. Montgomery, "Mechatronics by Bond Graphs", Springer, 2003.
- [3] Dean C. Karnopp, Donald L. Margolis and Ronald C. Rosenberg, "System Dynamics Modeling and Simulation of Mechatronic Systems", John Wiley & Sons, 2000.
- [4] P. E. Wellstead, "Physical System Modelling", Academic Press, London, 1979.
- [5] C. Sueur and G. Dauphin-Tanguy, "Bond graph approach for structural analysis of MIMO linear systems", Journal of the Franklin Institute, Vol. 328, No. 1, pp. 55-70, 1991.
- [6] Peter Gawthrop and L. Smith, "Metamodelling", Prentice-Hall, 1996.
- [7] M. J. L. Tiernego, J. J. Dixhoorn, "Three Axis Platform Simulation: Bond Graph and Lagrangian Approach", Journal of the Franklin Institute, Vol. 308, No. 1/2, pp. 157-171, 1985.
- [8] A. Zeid, Ch. H. Chung, "Bond Graph Modelling of Multibody System: a Library of Three dimensional Joints", Journal of the Franklin Institute, Vol. 329, No. 4, pp. 605-636, 1992.
- [9] D. Karnopp, "Understanding Multibody Dynamics using Bond Graph Representations", Journal of the Franklin Institute, Vol. 334B, No. 4, pp. 631-642, 1997.
- [10] L. M. Silverman, "Inversion of multivariable linear systems", IEEE Trans. Automat. Contr., Vol. AC-14, No. 3, pp. 270-276, June, 1969.
- [11] P. J. Gawthrop, "Bicausal bond graphs", in Proceedings of the 1995 International Conference on Bond Graph Modelling and Simulation: ICBGM'95, pp. 83-88, 1995.
- [12] R. Fotsu Ngwompo, S. Scavarda and D. Thomasset, "Inversion of Linear Time-invariant SISO Systems Modelled by Bond Graph", Journal of the Franklin Institute, Vol. 333(B), No. 2, pp. 157-174, 1996.
- [13] Gilberto Gonzalez-A and R. Galindo, "A Linearization Procedure for a Class of Nonlinear Systems Based on Bond Graph", Proceedings of the International Mediterranean Modeling Multiconference, pp. 77-82, 2005.